Neuron
Report

Regulation of Postsynaptic Retrograde Signaling by Presynaptic Exosome Release

Ceren Korkut,[1,2] Yihang Li,[1,2] Kate Koles,[1] Cassandra Brewer,[1] James Ashley,[1] Motojiro Yoshihara,[1] and Vivian Budnik[1,*]
[1]Department of Neurobiology, University of Massachusetts Medical School, Worcester, MA 01605, USA
[2]These authors contributed equally to this work
*Correspondence: vivian.budnik@umassmed.edu
http://dx.doi.org/10.1016/j.neuron.2013.01.013

SUMMARY

Retrograde signals from postsynaptic targets are critical during development and plasticity of synaptic connections. These signals serve to adjust the activity of presynaptic cells according to postsynaptic cell outputs and to maintain synaptic function within a dynamic range. Despite their importance, the mechanisms that trigger the release of retrograde signals and the role of presynaptic cells in this signaling event are unknown. Here we show that a retrograde signal mediated by Synaptotagmin 4 (Syt4) is transmitted to the postsynaptic cell through anterograde delivery of Syt4 via exosomes. Thus, by transferring an essential component of retrograde signaling through exosomes, presynaptic cells enable retrograde signaling.

INTRODUCTION

The *Drosophila* neuromuscular junction (NMJ) is a powerful system to investigate mechanisms underlying retrograde signaling (Keshishian and Kim, 2004). Spaced stimulation of *Drosophila* larval and embryonic NMJs results in potentiation of spontaneous (quantal) release (Ataman et al., 2008; Yoshihara et al., 2005) through a retrograde signaling mechanism requiring postsynaptic function of the vesicle protein Synaptotagmin 4 (Syt4) (Barber et al., 2009; Yoshihara et al., 2005).

Synaptotagmins are a family of membrane trafficking proteins composed of an N-terminal transmembrane domain, a linker sequence, and two C-terminal C2 domains (Chapman, 2008). The most abundant isoform in the nervous system, Synaptotagmin 1 is associated with synaptic vesicles and has been proposed to function as a Ca^{2+} sensor for neurotransmitter release (Chapman, 2008). Among Synaptotagmins, Syt4 (Littleton et al., 1999; Vician et al., 1995) occupies an interesting yet poorly understood position. Its expression is regulated by electrical activity (Babity et al., 1997; Vician et al., 1995), it is present in vesicles containing regulators of synaptic plasticity and growth, such as BDNF (Dean et al., 2009), it regulates learning and memory (Ferguson et al., 2001), and in humans the *syt4* gene is localized to a locus linked to schizophrenia and bipolar disorder (Ferguson et al., 2001).

At the fly NMJ, spaced stimulation results not only in potentiation of spontaneous neurotransmitter release (Ataman et al., 2008; Yoshihara et al., 2005) but also in structural changes at presynaptic arbors, the rapid formation of ghost boutons, nascent boutons that have still not developed postsynaptic specializations or recruited postsynaptic proteins (Ataman et al., 2008). However, whether this activity-dependent bouton formation also required Syt4-dependent retrograde signaling was unknown.

Here we demonstrate that retrograde Syt4 function in postsynaptic muscles is required for activity-dependent synaptic growth and that this function depends on exosomal release of Syt4 by presynaptic terminals.

RESULTS AND DISCUSSION

Postsynaptic Depolarization Is Required for Rapid Activity-Dependent Synaptic Growth

To determine whether, similar to the potentiation of spontaneous release (Barber et al., 2009; Yoshihara et al., 2005), the rapid formation of ghost boutons in response to spaced stimulation required retrograde signaling, we used an optogenetic approach to inhibit responses in the postsynaptic muscle cell. While body wall muscle preparations bathed in normal saline were stimulated after a spaced stimulation paradigm (Ataman et al., 2008), they were simultaneously hyperpolarized by activating the light-gated Cl^- channel Halorhodopsin (NpHR) (Zhang et al., 2007), which was expressed in muscles using the C57-Gal4 driver. Illuminating resting preparations expressing NpHR in muscle resulted in rapid hyperpolarization of the muscle membrane (Figure 1A). Using two electrode voltage clamp, we found that the NpHR current peaked at +46 ± 3.5 nA and decayed to +10.8 ± 1.18 nA within 2 min (n = 10). This was sufficient to induce an ~50% decrease in the amplitude of evoked excitatory junctional potentials (EJPs; Figures 1B and 1C; see Figure S1A available online; recorded in 0.5 mM Ca^{2+} saline), probably by shunting the depolarizing current induced by neurotransmitter release. This decrease in EJP amplitude was not due to a leaky UAS-NpHR transgene, because in the absence of Gal4 driver there was no significant change in EJP amplitude (Figure 1C; Figure S1A). A similar result has been previously reported when expressing the EKO K^+ channel in muscles (White et al., 2001).

Spaced stimulation of wild-type NMJs (lacking NpHR) in the presence or absence of light elicited a 3- to 4-fold increase in the number of ghost boutons (Figure 1D), which were labeled by the presynaptic membrane marker anti-HRP but lacked postsynaptic Discs-Large (DLG) (Figures 1E and 1F). Similarly,

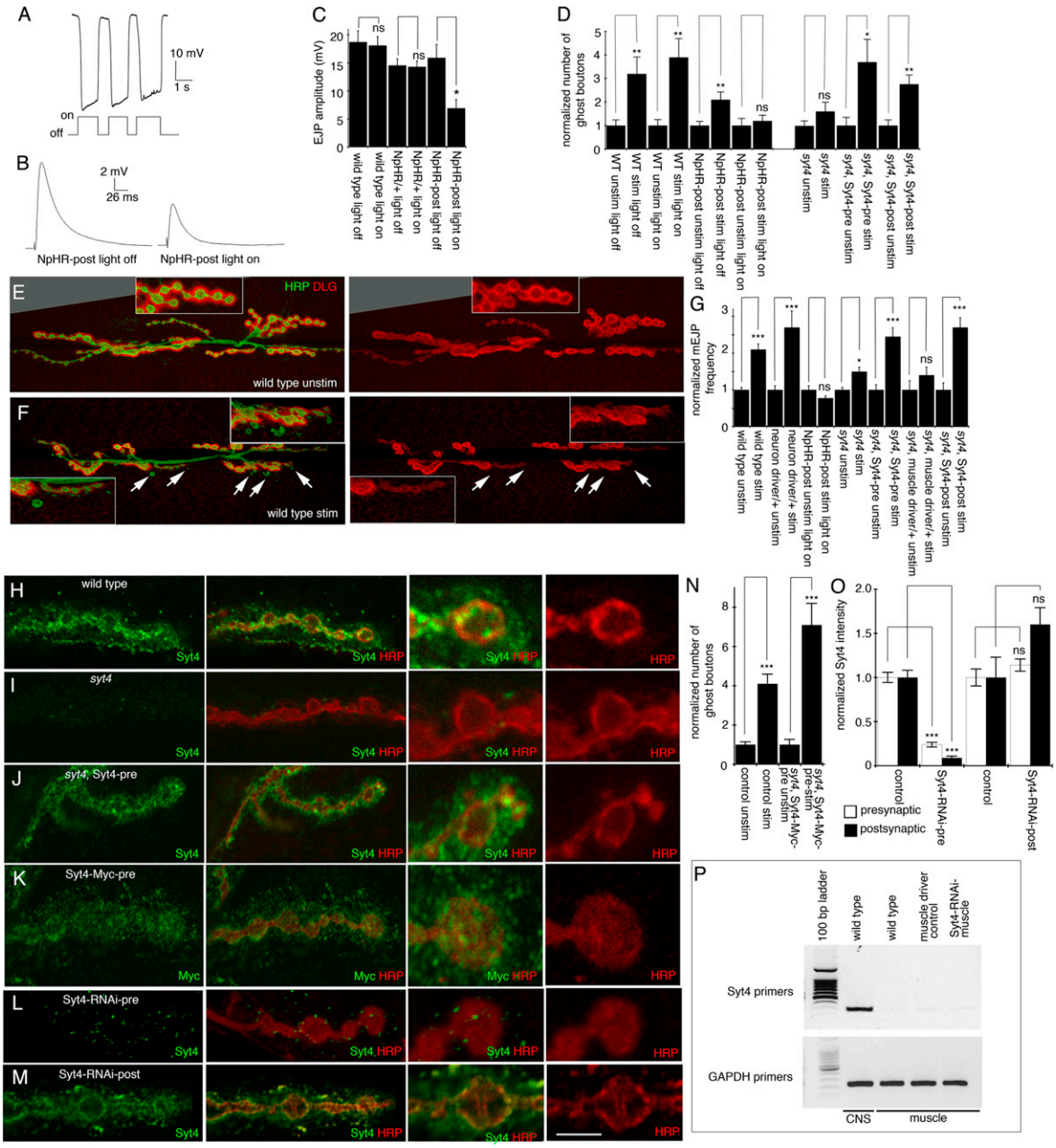

Figure 1. Retrograde Control of Synaptic Growth and Function by *trans*-Synaptic Syt4 Transfer

(A) Hyperpolarization of muscles (top trace) upon 560 nm illumination (bottom trace) in a third-instar larva expressing NpHR in muscle. (B) Nerve-evoked EJPs in control and upon activating NpHR in muscles. (C) Nerve-evoked EJP amplitude in wild-type, NpHR/+, and postsynaptic NpHR-expressing larvae. n (left to right) = 5, 5, 5, 5, 7, and 7, respectively. Also see Figure S1A. (D) Number of ghost boutons normalized to unstimulated controls induced after spaced stimulation of controls, animals expressing NpHR in *syt4* mutants and *syt4* rescue. n (left to right) = 14, 15, 11, 12, 27, 20, 16, 15, 28, 25, 15, 15, 15, and 13, respectively. (E and F) NMJs from third-instar larval muscles 6/7 (A3) labeled with anti-HRP and anti-DLG in wild-type unstimulated (E) and after spaced stimulation (F), showing ghost bouton (arrows) induction after stimulation. Insets show high magnification of NMJ branches. (G) mEJP frequency normalized to unstimulated controls. n (left to right) = 27, 30, 8, 9, 24, 26, 21, 23, 21, 21, 8, 8, 6, and 7, respectively. (H–M) Third-instar larval NMJ branches at muscles 6/7 (A3) shown at low (left two columns) or high (right two columns) magnification labeled with anti-HRP and anti-Syt4 (H–J, L, and M) or anti-Myc (K). Wild-type control (H); *syt4* null mutant (I); *syt4* null mutant expressing a wild-type Syt4 transgene in neurons (J); a larva expressing Syt4-Myc in neurons (K); also see Figures S1B and S1C; a larva expressing Syt4-RNAi in neurons (L); a larva expressing Syt4-RNAi in muscles (M). (N) Number of ghost boutons normalized to unstimulated controls in unstimulated and stimulated wild-type controls, as well as in unstimulated and stimulated *syt4* mutants expressing the Syt4-Myc transgene in neurons. n (left to right) = 15, 14, 21, and 15, respectively. (O) Syt4 immunoreactivity levels normalized to control levels. n (left to right) = 21, 12, 11, and 15, respectively. (P) RT-PCR from larval CNS and muscles showing Syt4 mRNA in neurons but not in muscles, with GAPDH mRNA as control. Calibration bar represents 20 μm in (E) and (F), 10 μm in insets, 6 μm in left two columns in (H)–(M), and 2.5 μm in right two columns in (H)–(M). ***$p < 0.001$; **$p < 0.01$; *$p < 0.05$. Error bars in plots represent mean ± SEM.

spaced stimulation of NMJs expressing NpHR in muscles in the absence of light resulted in a significant increase in the number of ghost boutons (Figure 1D). In contrast, light activation of NpHR in larval muscles completely blocked this effect (Figure 1D). Thus, postsynaptic depolarization is required for the formation of presynaptic ghost boutons in response to spaced stimulation, establishing that ghost bouton formation requires a retrograde signal.

Syt4 Is Required Either Pre- or Postsynaptically for Activity-Induced Ghost Bouton Formation and mEJP Potentiation

To determine whether Syt4 was required for the retrograde signal, we conducted the above experiments in *syt4* null mutants over a deficiency of the *syt4* locus, which prevented the formation of ghost boutons upon spaced stimulation (Figure 1D). If Syt4 was part of a retrograde signaling mechanism that regulates nascent bouton formation, then expressing Syt4 in postsynaptic muscles in a *syt4* mutant background should rescue the block in ghost bouton formation upon spaced stimulation. We expressed a wild-type Syt4 transgene in either muscles or neurons using the Gal4 drivers Mhc (Myosin heavy chain)-Gal4 (for muscles) and elav-Gal4 (for neurons). Surprisingly, expressing Syt4 in either muscles or neurons completely rescued the ability of NMJs to respond to spaced stimulation by forming ghost boutons (Figure 1D).

Previous studies at the larval NMJ suggested that the potentiation of miniature EJP (mEJP) frequency upon spaced stimulation was due to a Syt4-mediated retrograde signal, based on the observation that postsynaptic expression of Syt4 in a *syt4* null mutant background could rescue the lack of mEJP frequency potentiation upon stimulation (Barber et al., 2009). However, the ability of presynaptically expressed Syt4 to rescue this *syt4* mutant phenotype was not tested in this study. Given that *syt4* mutants were unable to form ghost boutons upon spaced stimulation and that this phenotype could be rescued either by pre- or postsynaptic Syt4 expression, we determined whether mEJP frequency potentiation could be rescued by expressing Syt4 in neurons and/or muscles of *syt4* mutants. Recording from body wall muscles after spaced stimulation (Ataman et al., 2008) demonstrated an over 2-fold increase in mEJP frequency in wild-type larvae (Figure 1G). This response was significantly reduced in *syt4* mutants (Figure 1G). Nevertheless, expressing Syt4 in either the neurons or muscles of *syt4* mutants completely rescued this phenotype (Figure 1G). Consistent with a requirement for retrograde signaling, blocking activity in the postsynaptic muscle using NpHR also completely blocked this response (Figure 1G). Thus, Syt4 is required either pre- or postsynaptically for activity-dependent ghost bouton formation and mEJP frequency potentiation at the larval NMJ, raising questions about a purely retrograde role of Syt4.

Syt4 Is Transferred *trans*-Synaptically from Presynaptic Boutons to Postsynaptic Muscle Compartments

As previously reported (Adolfsen et al., 2004), Syt4 is localized both in pre- and postsynaptic compartments of wild-type NMJs, as determined by double labeling with anti-HRP antibodies, which is used as a neuronal membrane marker to determine the boundary between presynaptic boutons and postsynaptic muscles (Figure 1H). The Syt4 signal was specific, as it was virtually eliminated in *syt4* null mutants (Figure 1I). Notably, expressing a Syt4 transgene exclusively in the neurons of *syt4* null mutants rescued both the presynaptic and postsynaptic localization of Syt4 (Figure 1J). This observation raises the possibility that presynaptic Syt4 might be transferred to the postsynaptic region and that postsynaptic Syt4 might at least be partly derived from presynaptic boutons. Consistent with this, expressing a C-terminally Myc-tagged Syt4 (Syt4-Myc) transgene in wild-type motor neurons using the OK6-Gal4 driver mimicked the endogenous localization of Syt4 in both presynaptic boutons and the postsynaptic muscle region (Figure 1K). The same postsynaptic localization of Syt4 was observed when expressing the transgene using either the neuronal Gal4 drivers elav-Gal4 or C380-Gal4 (Figures S1B and S1C). Like the wild-type, untagged transgene, presynaptically expressed Syt4-Myc completely rescued the *syt4* mutant phenotype upon spaced stimulation (Figure 1N), suggesting that the tagged transgene is functional. These observations suggest that endogenous Syt4 might be transferred from synaptic boutons to muscles.

This was tested by downregulating endogenous presynaptic Syt4 by expressing Syt4-RNAi in neurons. In agreement with the above model, downregulating Syt4 in motorneurons resulted in near elimination of the Syt4 signal, not only from presynaptic boutons but also from the postsynaptic muscle region (Figures 1L and 1O). Thus, the transfer of Syt4-Myc from neurons to muscles is not just the result of overexpressing the transgene in neurons but is probably an endogenous process. Further, although Syt4-RNAi was highly efficient at decreasing the Syt4 signal from motorneurons and muscles when expressed in motorneurons, expressing Syt4-RNAi in muscles using the strong C57-Gal4 driver did not decrease Syt4 levels in either the pre- or postsynaptic compartment (Figures 1M and 1O). These results support the idea that at least an important fraction of, if not all, postsynaptic Syt4 is derived from presynaptic neurons.

We also determined whether neurons and/or muscles contained *syt4* transcripts. RT-PCR using equal amounts of total RNA derived from either the nervous system or body wall muscles revealed the presence of a strong *syt4* band in the nervous system (Figure 1P). However, virtually no *syt4* transcript was observed in the muscles of wild-type controls or larvae expressing Syt4-RNAi in muscles (Figure 1P). This is again consistent with the possibility that muscle Syt4 might be exclusively derived from the transfer of neuronal Syt4 by synaptic boutons.

Syt4 Traffics in a Manner Similar to Evi at the NMJ

Syt4 is a transmembrane protein (Littleton et al., 1999; Vician et al., 1995), and thus its transfer from pre- to postsynaptic cells is not possible through classical vesicle exocytosis. However, we have previously observed the intercellular transfer of a transmembrane protein through exosome vesicles at the NMJ (Koles et al., 2012; Korkut et al., 2009), a process also observed in the immune system (Théry et al., 2009). In particular, the release and extracellular trafficking of hydrophobic Wnt-1 molecules at the NMJ appears to be mediated by Wnt binding to a multipass

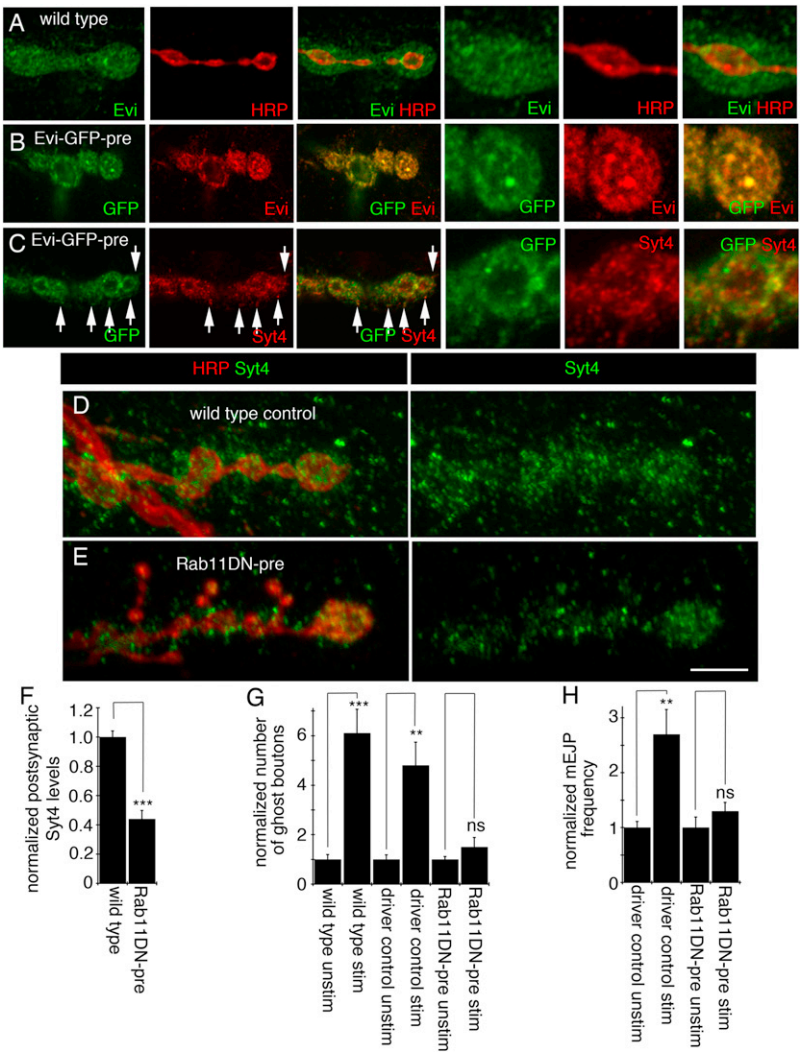

Figure 2. Syt4 and Evi Partially Colocalize at the NMJ and Interfering with Rab11 Function in Neurons Inhibits Syt4 Transfer from Pre- to Postsynaptic Compartments as Well as Retrograde Signaling

(A–E) Third-instar larval NMJs at muscles 6 or 7 (A3) in wild-type (A), larvae expressing Evi-GFP in neurons (B and C), neuronal driver control (D), and larvae expressing Rab11DN in neurons (E), labeled with anti-Evi and anti-HRP(A), anti-GFP and anti-Evi (B), and anti-GFP and anti-Syt4 (C). Arrows represent colocalization of transgenic Evi and endogenous Syt4. (D and E) Anti-Syt4 and anti-HRP. Also see Figures S2A and S2B. Calibration bar represents 9 μm in left panels in (A)–(C) and 5 μm in right panels in (A)–(C) and in (D) and (E). (F) Normalized postsynaptic Syt4 levels. n (left to right) = 25 and 25, respectively. (G) Number of ghost boutons normalized to unstimulated preparations in controls and animals expressing Rab11DN in neurons. n (left to right) = 20, 21, 15, 10, 16, and 12, respectively. (H) mEJP frequency normalized to unstimulated preparations in controls and larvae expressing Rab11DN in neurons. n (left to right) = 6, 9, 6, and 8, respectively.

transmembrane protein, Evi/Wls, which is released to the extracellular space in the form of exosomes (Koles et al., 2012; Korkut et al., 2009). Exosomes are vesicles generated by the inward budding of endosomal limiting membrane into multivesicular bodies (MVBs). MVBs can either fuse with lysosomes to dispose of obsolete cellular material or with the plasma membrane to release vesicle-associated signaling components (Simons and Raposo, 2009).

The similar transfer of transmembrane Evi and Syt4 across cells raised the possibility that like Evi, Syt4 could be secreted through exosomes, perhaps the same exosome. To address this possibility, we first determined the extent of Evi and Syt4 colocalization at the NMJ. Neuronally expressed Evi-GFP has a similar distribution pattern to that of endogenous Evi (Figures 2A and 2B), and the Evi-GFP transgene is functional, as it can rescue all mutant phenotypes in *evi* mutants (Korkut et al., 2009). Given that antibodies to Syt4 and Evi were raised in the same species, we expressed Evi-GFP in motorneurons and visualized the colocalization of the GFP label with endogenous Syt4. The colocalization of the GFP and Syt4 signal was not complete (Figure 2C). However, several of the postsynaptic GFP-positive puncta also contained endogenous Syt4 signal (Figure 2C, arrows). Whether these puncta correspond to single exosomes, a group of exosomes, or exosomes that have fused to an intracellular compartment cannot be determined by confocal microscopy, as exosomes are 50–100 nm in diameter.

Nevertheless, we previously demonstrated that Rab11 is required for Evi-exosome release from presynaptic terminals (Koles et al., 2012). Thus, we expressed a dominant-negative form of Rab11 (Rab11DN) in neurons and examined the levels of postsynaptic Syt4. We found that, as in the case of Evi (Koles et al., 2012), expression of Rab11DN in neurons drastically decreased the levels of endogenous postsynaptic Syt4 (Figures 2D–2F). Most notably, interfering with Rab11 in neurons completely suppressed activity-dependent ghost bouton formation (Figure 2G) and mEJP potentiation (Figure 2H). Thus, Syt4 transfer from neurons to muscles is likely to involve exosomes and these presynaptically derived exosomes are required for retrograde signaling.

In contrast to Rab11, Evi was not required for the release of Syt4, because in *evi* mutants, levels of postsynaptic Syt4 were normal (Figure S2B). Similarly, Evi levels were normal at the postsynaptic compartment of *syt4* null mutant (Figure S2A), suggesting that while Evi is (Koles et al., 2012), and Syt4 might be, an exosomal cargo, they are not required for exosomal release.

Interestingly, when both transgenic Syt4-Myc and Evi-GFP were overexpressed in neurons, both proteins became trapped in a compartment inside synaptic boutons, where they colocalized with hepatocyte growth factor (HGF)1-regulated tyrosine kinase substrate (HRS), which is often associated with endosomes (Komada et al., 1997) (Figures 3A and 3B). The mechanisms by which both proteins become trapped at

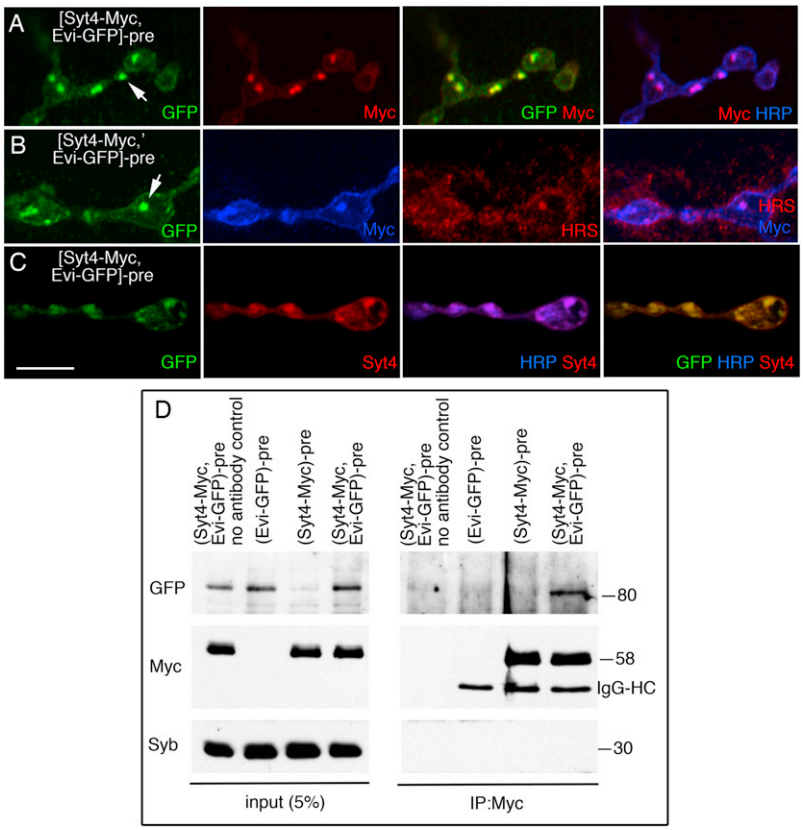

Figure 3. Trapping Syt4 in Presynaptic Boutons Reveals Absence of Endogenous Syt4 in Postsynaptic Muscles

(A–C) Third-instar larval NMJ branches at muscles 6 or 7 (A3) in larvae expressing both Evi-GFP and Syt4-Myc in neurons labeled with antibodies to GFP, Myc, and HRP (A); GFP, Myc, and HRS (B); GFP, Syt4 (labeling both endogenous and transgenic Syt4), and HRP (C). Calibration bar represents 6.5 μm. (D) Coimmunoprecipitation of Evi-GFP by Myc antibodies from body wall muscle and CNS extracts obtained from larvae expressing both Evi-GFP and Syt4-Myc in neurons. Numbers at the right represent molecular weight in kDa. IgG-HC, IgG heavy chain. Also see Figures S3A–S3C.

presynaptic terminals are unclear, but it might result from defects in trafficking when the proteins are overexpressed. Most importantly, labeling the NMJs of animals overexpressing both Syt4 and Evi using Syt4 antibodies, which should label both endogenous and transgenically expressed Syt4, revealed that the entire Syt4 protein pool accumulated in HRS-positive compartments inside presynaptic boutons and that no detectable Syt4 signal was observed at the postsynaptic region (Figure 3C). Taken together, the observation that *syt4* transcript is virtually absent in muscles, the ability of presynaptically driven Syt4-RNAi to eliminate Syt4 protein in postsynaptic muscles, and the finding that trapping Syt4 within presynaptic HRS-positive compartments completely eliminates postsynaptic Syt4 immunoreactivity provide compelling evidence that Syt4 protein is synthesized in larval neurons and not in larval muscles. It also suggests a mechanism similar to the *trans*-synaptic trafficking of Evi, through the release of exosomes (Koles et al., 2012; Korkut et al., 2009).

The trapping of Evi and Syt4 in an intracellular neuronal compartment when the proteins were overexpressed raised the possibility that the proteins may form a biochemical complex during trafficking. This was tested by coexpressing Syt4-Myc and Evi-GFP in the neurons of larvae to immunoprecipitate Syt4-Myc from body wall muscle and CNS extracts using Myc antibodies. Myc antibodies specifically immunoprecipitated Evi-GFP in vivo (Figure 3D). In contrast, the vesicle protein Neuronal Synaptobrevin (n-Syb) (DiAntonio et al., 1993) did not coprecipitate with Evi-GFP and Syt4-Myc (Figure 3D). We were also able to consistently coprecipitate Evi-GFP with endogenous Syt4 at the NMJ using a chicken Syt4 antibody (Figures S3A–S3C). However, the coprecipitation was weak (Figure S3C). Taken together with the lack of complete colocalization, this result suggests that an interaction between Syt4 and Evi might not be the dominant state of the proteins within the cell (also see below).

The *trans*-Cellular Transfer of Syt4 Is through Exosomes

To determine whether Syt4 could be found in the exosome fraction of S2 cells, we processed purified exosomes derived from a stable S2 cell line expressing Syt4-HA for immunoelectron microscopy. Since the HA tag is expected to be present within the lumen of exosomes, we developed a protocol for immunolabeling exosome luminal antigens. Briefly, purified exosomes were gently permeabilized with 0.05% saponin for 10 min, and after primary antibody incubation, a nanogold-conjugated secondary antibody was used, followed by silver intensification. We detected either the GFP tag at the C terminus of Evi inside exosomes derived from Evi-GFP S2 cells (Figure 4A) or the HA tag in exosomes derived from Syt4-HA S2 cells (Figure 4B; see Figure S4 for control), consistent with the model that Syt4 is present in exosomes. The gold label was observed either inside or at the outer edge of exosomes, which is commensurate with the size of the primary/secondary antibody complex (20–30 nm).

Specific transfer of Evi-exosomes from cell to cell has been demonstrated between nonneuronal S2 cells (Koles et al., 2012; Korkut et al., 2009). To determine whether similar transfer of Syt4 could be observed, we separately transfected S2 cells with either Syt4-V5 or mCherry. Then, Syt4-V5 and mCherry S2 cells were coincubated in the same culture dish. We observed that Syt4-V5 puncta were transferred to mCherry S2 cells (Figures 4C and 4D), consistent with our observations at the NMJ.

To determine whether some of the Evi and Syt4 could be sorted to the same exosome, S2 cells were cotransfected with tagged Evi and Syt4. Transfer of tagged Evi and Syt4 puncta into untransfected cells was observed (Figure 4E). However,

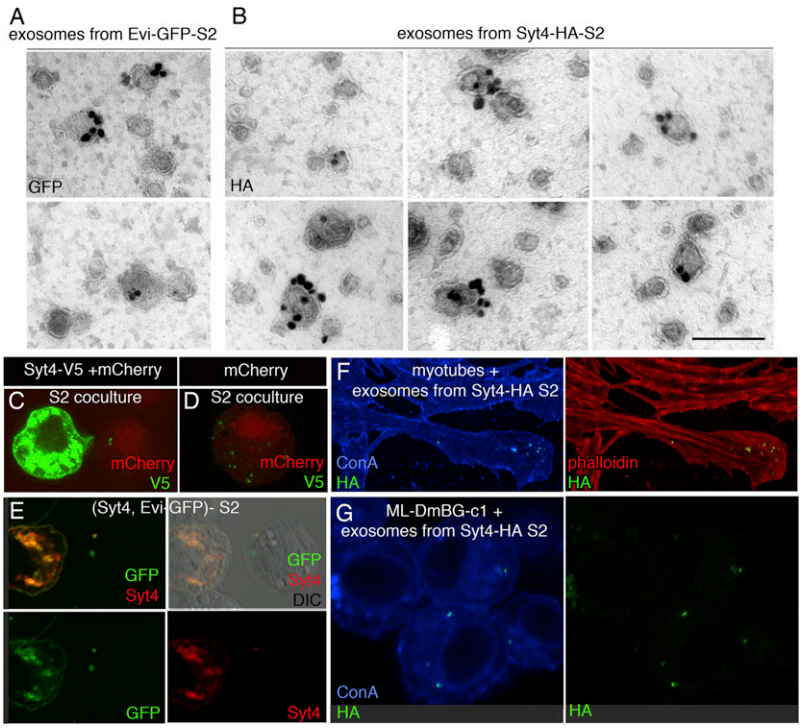

Figure 4. Syt4 Is Present in Purified S2 Cell Exosomes and Purified Exosomes from Syt4-HA S2 Cells Are Taken Up by S2 Cells, Primary Myoblast Cell Cultures, and a Neuronal Cell Line

(A and B) Electron micrographs of purified, permeabilized, and negatively stained exosome fraction from the culture medium of Evi-GFP-S2 cells labeled with anti-GFP (A) and Syt4-HA-S2 cells labeled with anti-HA (B). Also see Figure S4. (C–E) S2 cells labeled with anti-V5 and mCherry in cocultures of Syt4-V5-S2 and mCherry-S2 cells (C and D). In (C), both a Syt4-V5-transfected and an mCherry-transfected cell are observed. Note that V5-positive puncta are visualized within the mCherry cell, suggesting that Syt4-V5 is transferred transcellularly. In (D), an mCherry cell from the coculture in (C) is shown, demonstrating the presence of transferred Syt4-V5 puncta. In (E), the transfer of Evi-GFP- and/or Syt4-containing puncta to an untransfected cell, from S2 cells coexpressing Evi-GFP and untagged Syt4, is shown. (F and G) Confocal image of myotubes from gastrula embryos (F) and cells from a *Drosophila* neuronal cell line (G), incubated with purified exosome fraction from Syt4-HA-S2 cells, labeled with fluorescently conjugated concanavalin A (ConA) to stain membranes (F and G), and anti-HA, as well as fluorescent phalloidin to label myofibrils (F). Calibration bar represents 0.17 μm in (A) and (B), 12 μm in (C)–(E), 15 μm in (F), and 8 μm in (G).

most puncta contained either Syt4 alone (63.4% ± 7.4% of transferred puncta) or Evi alone (23% ± 6.3% of transferred puncta), and only in 13.2% ± 1.9% of the transferred puncta were Evi and Syt4 found together (n = 5 independent experiments, 2 experiments with Evi-V5 and Syt4-Dendra cotransfection and 3 with Evi-GFP and Syt4-Myc cotransfection; cotransfection efficiency = 69.4% ± 8.1%). Thus, although Evi and Syt4 can be packaged together, most of the time they exist in independent puncta. This is also consistent with the observation that the interaction between Evi and Syt4 is relatively weak or represents just a small portion of the entire Evi and Syt4 protein pool.

We also determined whether other cultured cell types were able to take up Syt4 exosomes. In particular, cultured myotubes derived from gastrula embryos (Bai et al., 2009) and a third-instar neuronal cell line, CNS ML-DmBG1-c1 (Ui et al., 1994), were able to take up Syt4-containing exosomes purified from Syt4-HA S2 cells (Figures 4F and 4G). Together with the observation that Syt4 is transferred from presynaptic compartments to postsynaptic muscle cells in vivo and that purified Syt4-containing exosomes are taken up by S2 cells as well as cultured primary muscle cells and neurons, these results strongly suggest that Syt4-containing exosomes are transferred transcellularly. Nevertheless, the presence of other nonexosomal mechanisms of transcellular Syt4 transport, such as cytonemes (Roy et al., 2011), cannot be ruled out.

In conclusion, we show that Syt4 protein functions in postsynaptic muscles to mediate activity-dependent presynaptic growth and potentiation of quantal release. However, to mediate this function, Syt4 needs to be transferred from presynaptic terminals to postsynaptic muscle sites. We present evidence that, most likely, the entire pool of postsynaptic Syt4 is derived from presynaptic cells. We also show that like the Wnt binding protein Evi, Syt4 is packaged in exosomes, which provides a mechanism for the unusual transfer of transmembrane proteins across cells. Taken together, our studies support a significant mechanism for the presynaptic control of a retrograde signal, through the presynaptic release of exosomes containing Syt4.

Larval NMJs continuously generate new synaptic boutons and their corresponding postsynaptic specializations (Koon et al., 2011; Zito et al., 1999), ensuring constant synaptic efficacy despite the continuous growth of muscle cells (Li et al., 2002). This precise matching of pre- and postsynaptic compartments is regulated by electrical activity (Budnik et al., 1990), which induces a retrograde signal in muscle to stimulate new presynaptic growth. This process is likely to fine-tune the magnitude of the retrograde signal in specific nerve terminal-muscle cell pairs, each with a characteristic size. Given that most larval muscle cells are innervated by multiple motorneurons, this mechanism may also enable spatial coincidence to ensure the synaptic specificity of plasticity, making certain that only those activated synapses within a cell become structurally regulated (Yoshihara et al., 2005).

EXPERIMENTAL PROCEDURES

See a detailed description in the Supplemental Experimental Procedures.

Fly Strains

We used wild-type (Canton-S); *syt4*^{BA1}; *rn*^{16} (deficiency of the Syt4 locus); UAS-Syt4; UAS-Syt4-RNAi; UAS-Evi-GFP; *evi*^{2}; UAS-Syt4-Myc; UAS-eNpHR3.0-EYFP; UAS-Rab11DN^{N124I}, C155-Gal4; C380-Gal4; C57-Gal4; Mhc-Gal4; and OK6-Gal4.

Immunocytochemistry

Third-instar larval body wall muscles were processed for immunocytochemistry as in Ataman et al. (2008). Antibodies used are specified in the Supplemental Experimental Procedures.

Image Acquisition and Quantification

Confocal images were acquired using a Zeiss LSM5 Pascal confocal microscope with a Zeiss 63× Plan-Apochromat (1.4 numerical aperture) DIC with oil-immersion objective at 3× digital zoom. Signal intensity was quantified by volumetric measurements of confocal stacks using Volocity 5 Software (Improvision) as described in Korkut et al. (2009).

Spaced Stimulation

Spaced K^+ stimulation was performed as in Ataman et al. (2008).

Electrophysiology

Spaced and sham stimulation were performed as above, and then samples were prepared for electrophysiology as in Ataman et al. (2008). Voltage clamp was performed as in Gorczyca et al. (2007). Passive properties were determined as in Haugland and Wu (1990). There was no significant difference in these properties between genotypes examined.

S2 Cell Transfection and Immunocytochemistry

S2 cells were cultured at 25°C in SFX insect medium (HyClone) containing 10% fetal bovine serum (FBS) (HyClone), penicillin (50 U/ml), and streptomycin (50 μg/ml) (Sigma) and maintained in Nunclon Δ Surface T-flasks (Thermo Scientific). For immunocytochemistry, cells were plated on 6-well Nunclon plates (Thermo Scientific) and at 60%–80% confluency they were transfected with 0.5 μg DNA using Effectene transfection kit (QIAGEN).

Exosome Preparation

Exosomes were prepared as in Lässer et al. (2012) with slight modifications from stably transfected Evi-GFP- (Koles et al., 2012) or Syt4-HA S2 cells. Cells were cultured as above but without FBS and were pelleted by centrifugation at 600 × *g* for 10 min. The supernatant was then cleared of larger debris by centrifugation at 16,500 × *g* for 20 min and passed through a 0.22 μm filter, and exosomes were pelleted at 120,000 × *g* for 75 min. The pellet was resuspended in minimal volume of 100 mM Tris (pH 7.4) and kept at −80°C until further use or fixed overnight in 2% paraformaldehyde for immunoelectron microscopy.

Exosome Uptake

Gastrula embryos were dechorionated, homogenized in Shields and Sang medium containing 15% FBS, 10 μg/ml insulin, and penicillin/streptomycin, and plated on coverslips. These were cultured for 2 days at 22°C before addition of Syt4-HA exosomes for 2 hr. The ML-DmBG1-c1 larval neuron cell line was cultured at 27°C according to DGRC guidelines and incubated with purified Syt4-HA exosomes for 2 hr.

Immunoelectron Microscopy of Exosomes

Exosomes were fixed in 2% paraformaldehyde at 4°C overnight and spotted onto formvar-coated Nickel grids (200 mesh). Grids were immunolabeled after exosome permeabilization with saponin and negatively stained as described in Koles et al. (2012).

Immunoprecipitation and Western Blotting

Third-instar larvae were dissected in ice-cold Ca^{2+}-free saline, and body wall muscles and CNS were homogenized. For coimmunoprecipitation of S2 cell extracts, cells were harvested and lysed prior to immunoprecipitation.

RT-PCR

Total RNA was extracted from larval body wall muscles (without CNS) or larval brains in Trizol (Invitrogen) at 4°C and purified with the RNeasy Micro Kit (QIAGEN). cDNA was synthesized using a SuperScriptIII Kit (Invitrogen).

Syt4 Antibodies

Affinity-purified anti-Syt4 was raised by New England peptide by immunizing chickens with the peptides KYSEEGDGPAQHAEQC and SKEIQPRSLKIRAC.

Molecular Biology

We generated pUAST-Syt4-Myc, pAc-Syt4-V5, pUAST-attB-Syt4-HA-sp11 (herein named Syt4-HA), pUAST-Syt4-Dendra2, and pUAST-eNpHR3.0-EYFP.

SUPPLEMENTAL INFORMATION

Supplemental Information includes four figures and Supplemental Experimental Procedures and can be found with this article online at http://dx.doi.org/10.1016/j.neuron.2013.01.013.

ACKNOWLEDGMENTS

We thank members of the Budnik laboratory for helpful discussions. We also thank Dr. Troy Littleton, Dr. Michael Boutros, Dr. Patrick Emery, Dr. Carl Deisseroth, and the Vienna *Drosophila* RNAi Center for generous reagent sharing. We thank John Nunnari and the core electron microscopy facility at UMass Medical School. This work was supported by NIH grants MH070000 to V.B. and MH85958 to M.Y. Authors contribution is as follows: C.K. carried out most of the experiments, generated the chicken Syt4 antibody, coordinated the project, contributed intellectually to experimental design and interpretation, and contributed to writing the manuscript; Y.L. carried out immunoprecipitations and anatomical analysis, contributed intellectually to experimental design and interpretation, and coordinated the project in its last stages; C.B. carried out electrophysiological experiments; K.K. performed the purification of the exosomal fraction, immunoelectron microscopy of exosomes, and exosome uptake assays in myotubes from gastrula embryos and the CNS cell line; J.A. carried out electrophysiology and immunoelectron microscopy; M.Y. contributed to the initial observation of *trans*-synaptic Syt4 transfer, generation of the chicken Syt4 antibody, and to helpful discussions; and V.B. directed the project, experimental design, and interpretations and wrote the manuscript.

Accepted: January 4, 2013
Published: March 20, 2013

REFERENCES

Adolfsen, B., Saraswati, S., Yoshihara, M., and Littleton, J.T. (2004). Synaptotagmins are trafficked to distinct subcellular domains including the postsynaptic compartment. J. Cell Biol. *166*, 249–260.

Ataman, B., Ashley, J., Gorczyca, M., Ramachandran, P., Fouquet, W., Sigrist, S.J., and Budnik, V. (2008). Rapid activity-dependent modifications in synaptic structure and function require bidirectional Wnt signaling. Neuron *57*, 705–718.

Babity, J.M., Armstrong, J.N., Plumier, J.C., Currie, R.W., and Robertson, H.A. (1997). A novel seizure-induced synaptotagmin gene identified by differential display. Proc. Natl. Acad. Sci. USA *94*, 2638–2641.

Bai, J., Sepp, K.J., and Perrimon, N. (2009). Culture of Drosophila primary cells dissociated from gastrula embryos and their use in RNAi screening. Nat. Protoc. *4*, 1502–1512.

Barber, C.F., Jorquera, R.A., Melom, J.E., and Littleton, J.T. (2009). Postsynaptic regulation of synaptic plasticity by synaptotagmin 4 requires both C2 domains. J. Cell Biol. *187*, 295–310.

Budnik, V., Zhong, Y., and Wu, C.F. (1990). Morphological plasticity of motor axons in Drosophila mutants with altered excitability. J. Neurosci. *10*, 3754–3768.

Chapman, E.R. (2008). How does synaptotagmin trigger neurotransmitter release? Annu. Rev. Biochem. *77*, 615–641.

Dean, C., Liu, H., Dunning, F.M., Chang, P.Y., Jackson, M.B., and Chapman, E.R. (2009). Synaptotagmin-IV modulates synaptic function and long-term potentiation by regulating BDNF release. Nat. Neurosci. *12*, 767–776.

DiAntonio, A., Burgess, R.W., Chin, A.C., Deitcher, D.L., Scheller, R.H., and Schwarz, T.L. (1993). Identification and characterization of Drosophila genes for synaptic vesicle proteins. J. Neurosci. *13*, 4924–4935.

Ferguson, G.D., Vician, L., and Herschman, H.R. (2001). Synaptotagmin IV: biochemistry, genetics, behavior, and possible links to human psychiatric disease. Mol. Neurobiol. *23*, 173–185.

Gorczyca, D., Ashley, J., Speese, S., Gherbesi, N., Thomas, U., Gundelfinger, E., Gramates, L.S., and Budnik, V. (2007). Postsynaptic membrane addition depends on the Discs-Large-interacting t-SNARE Gtaxin. J. Neurosci. *27*, 1033–1044.

Haugland, F.N., and Wu, C.F. (1990). A voltage-clamp analysis of gene-dosage effects of the Shaker locus on larval muscle potassium currents in Drosophila. J. Neurosci. *10*, 1357–1371.

Keshishian, H., and Kim, Y.S. (2004). Orchestrating development and function: retrograde BMP signaling in the Drosophila nervous system. Trends Neurosci. *27*, 143–147.

Koles, K., Nunnari, J., Korkut, C., Barria, R., Brewer, C., Li, Y., Leszyk, J., Zhang, B., and Budnik, V. (2012). Mechanism of evenness interrupted (Evi)-exosome release at synaptic boutons. J. Biol. Chem. *287*, 16820–16834.

Komada, M., Masaki, R., Yamamoto, A., and Kitamura, N. (1997). Hrs, a tyrosine kinase substrate with a conserved double zinc finger domain, is localized to the cytoplasmic surface of early endosomes. J. Biol. Chem. *272*, 20538–20544.

Koon, A.C., Ashley, J., Barria, R., DasGupta, S., Brain, R., Waddell, S., Alkema, M.J., and Budnik, V. (2011). Autoregulatory and paracrine control of synaptic and behavioral plasticity by octopaminergic signaling. Nat. Neurosci. *14*, 190–199.

Korkut, C., Ataman, B., Ramachandran, P., Ashley, J., Barria, R., Gherbesi, N., and Budnik, V. (2009). Trans-synaptic transmission of vesicular Wnt signals through Evi/Wntless. Cell *139*, 393–404.

Lässer, C., Eldh, M., and Lötvall, J. (2012). Isolation and characterization of RNA-containing exosomes. J. Vis. Exp. (59), e3037.

Li, H., Peng, X., and Cooper, R.L. (2002). Development of Drosophila larval neuromuscular junctions: maintaining synaptic strength. Neuroscience *115*, 505–513.

Littleton, J.T., Serano, T.L., Rubin, G.M., Ganetzky, B., and Chapman, E.R. (1999). Synaptic function modulated by changes in the ratio of synaptotagmin I and IV. Nature *400*, 757–760.

Roy, S., Hsiung, F., and Kornberg, T.B. (2011). Specificity of Drosophila cytonemes for distinct signaling pathways. Science *332*, 354–358.

Simons, M., and Raposo, G. (2009). Exosomes—vesicular carriers for intercellular communication. Curr. Opin. Cell Biol. *21*, 575–581.

Théry, C., Ostrowski, M., and Segura, E. (2009). Membrane vesicles as conveyors of immune responses. Nat. Rev. Immunol. *9*, 581–593.

Ui, K., Nishihara, S., Sakuma, M., Togashi, S., Ueda, R., Miyata, Y., and Miyake, T. (1994). Newly established cell lines from Drosophila larval CNS express neural specific characteristics. In Vitro Cell. Dev. Biol. Anim. *30A*, 209–216.

Vician, L., Lim, I.K., Ferguson, G., Tocco, G., Baudry, M., and Herschman, H.R. (1995). Synaptotagmin IV is an immediate early gene induced by depolarization in PC12 cells and in brain. Proc. Natl. Acad. Sci. USA *92*, 2164–2168.

White, B., Osterwalder, T., and Keshishian, H. (2001). Molecular genetic approaches to the targeted suppression of neuronal activity. Curr. Biol. *11*, R1041–R1053.

Yoshihara, M., Adolfsen, B., Galle, K.T., and Littleton, J.T. (2005). Retrograde signaling by Syt 4 induces presynaptic release and synapse-specific growth. Science *310*, 858–863.

Zhang, F., Wang, L.P., Brauner, M., Liewald, J.F., Kay, K., Watzke, N., Wood, P.G., Bamberg, E., Nagel, G., Gottschalk, A., and Deisseroth, K. (2007). Multimodal fast optical interrogation of neural circuitry. Nature *446*, 633–639.

Zito, K., Parnas, D., Fetter, R.D., Isacoff, E.Y., and Goodman, C.S. (1999). Watching a synapse grow: noninvasive confocal imaging of synaptic growth in Drosophila. Neuron *22*, 719–729.